Compact high-speed snapshot multispectral imagers in the VIS/NIR (460 to 960 nm) and SWIR range (1.1 to 1.65 nm) and its potential in a diverse range of applications

C. Blanch-Perez-del-Notario, B. Geelen, Y. Li, R. Vandebriel, J. Bentell, et al.

C. Blanch-Perez-del-Notario, B. Geelen, Y. Li, R. Vandebriel, J. Bentell, M. Jayapala, W. Charle, "Compact high-speed snapshot multispectral imagers in the VIS/NIR (460 to 960 nm) and SWIR range (1.1 to 1.65 nm) and its potential in a diverse range of applications," Proc. SPIE 12338, Hyperspectral Imaging and Applications II, 1233806 (11 January 2023); doi: 10.1117/12.2664944

SPIE.

Event: SPIE Photonex, 2022, Birmingham, United Kingdom

Compact high-speed snapshot multispectral imagers in the VIS/NIR (460-960 nm) and SWIR range (1.1-1.65 nm) and its potential in a diverse range of applications

C. Blanch-Perez-del-Notario[a], B. Geelen[a], Y. Li[a], R. Vandebriel[a], J. Bentell[a], M. Jayapala[a] and W. Charle[a]

[a]Imec, Kapeldreef 75, 3001, Leuven, Belgium

ABSTRACT

This paper presents the latest advances on Imec snapshot multispectral imagers based on either 3x3, 4x4 and 5x5 mosaic filter patterning on industry ready VIS/NIR and SWIR detectors. The mosaic patterns are implemented by means of high-transmission Fabry-Pérot interferometers processed using thin-film technology. Our snapshot multispectral imagers offer a spatial resolution of 640x480 pixels (SWIR) and 2048x1088 (VIS/NIR) down sampled according to the mosaic pattern to acquire data in 9 (3x3), 16 (4x4) of 25 (5x5) spectral bands respectively. To achieve imaging at the native spatial resolution of the sensor, super resolution methods are available post-acquisition. Moreover, our compact USB-3 cameras of 260 gr (SWIR) and 27 gr (VNIR), without lens, reach an acquisition speed of up to 120 multispectral cubes/second and are therefore suitable for dynamic applications, high-speed inspection such as a conveyor belt or UAV inspection. The potential for snapshot cameras in a wide range of applications is showcased in this paper. We first show how applications on industrial quality inspection (chocolate gloss estimation) and precision agriculture (plant disease detection) achieve good discrimination potential in the VNIR range. Specifically, UAV inspection benefits from our compact camera size, low weight, and video capabilities. We then demonstrate the potential for plastic and textile recycling in the SWIR range and the benefit brought by both VNIR and SWIR ranges for people tracking under low visibility conditions. Finally, an application involving the joint use of a microscope and a multispectral camera system is presented for particle contamination exposure assessment. The suitable range is in this case application dependent.

Keywords: compact multispectral snapshot camera, high-speed video, VIS/NIR range, SWIR range, sorting, agriculture, medical, industrial inspection, microscopy, object tracking.

1. INTRODUCTION

Hyperspectral imaging combines the characteristics of computer vision and point spectroscopy by obtaining an image with both spatial and spectral information. This technique enables therefore to analyse the chemical composition of materials while visualizing their spatial distribution [1], with its key advantages being that it is a non-invasive, non-contact and non-destructive technology. There are many applications where hyperspectral imaging has gained high interest in the recent years: namely food inspection, forensic science, medical surgery and diagnosis and military applications [2]. This growing interest was fuelled by technological advances in hyperspectral instrumentation as well as in computer technology. Hyperspectral cameras of lower size and cost factor providing faster acquisition and increased resolution have become available in the last decade [3]. In addition, processing devices are becoming increasingly more powerful to process the large amount of hyperspectral data [4]. Finally, the recent advances in machine learning and deep learning are increasing the means to process these images [5]. Hyperspectral image data can be acquired in different ways, known as spatial scanning, spectral/wavelength scanning, spatio-spectral scanning, and non-scanning (or snapshot) imaging [6]. In spatial scanning, each two-dimensional sensor output corresponds to a full slit spectrum. A strip of the scene is projected onto a slit, which is dispersed by a prism or a grating. The image is acquired line by line in a push broom manner [7], and a scanning movement is required to capture a full hyperspectral 3d cube.

*carolina.blanch@imec.be; phone 32 281008; imec.be

Hyperspectral Imaging and Applications II, edited by Nick J. Barnett, Aoife A. Gowen, Haida Liang, Proc. of SPIE Vol. 12338, 1233806
 · 0277-786X · doi: 10.1117/12.2664944

Traditional hyperspectral cameras performing spatial scanning are based on a prism grating systems. In spectral scanning, the full image is acquired for an individual waveband at a time. This way, each 2-D sensor output represents a single band image of the scene. These devices are typically based on optical band-pass filters, which can be tunable or fixed. An example of such system is a filter wheel system, where a rotating wheel is synchronized with the camera acquisition per filter. Such systems offer a reduced number of filters, and their acquisition speed is limited to the mechanical rotation speed. The two most used electronically tunable filters are liquid crystal tunable filters (LCTF) and acousto-optical tunable filters (AOTF). Hyperspectral imaging techniques based on these type of filters [8] require polarized light to achieve spectral selectivity. This limits their use in low light applications, since their throughput is at most 40%, lower than the 60–90% typical for thin film band-pass filters. Spatio-spectral scanning produces a series of thin, diagonal slices of the data cube. Each acquired image is a 'rainbow-colored' spatial map of the scene, where different lines correspond to different wavelength responses. This way, scanning is required to acquire the spectrum of a given object point. Examples of spatio-spectral scanning systems are Imec line-scan [9] and Snapscan camera systems [10]. An example of a tunable filter system is the hyperspectral camera concept described in [11], where a Continuous Variable Filter (CVF), a.k.a Linear Variable Filter (LVF) of Delta Film [12] is used. The 18 bands in the VNIR range are acquired with the translational movement of the UAV and used to reconstruct the 3D structure in the scene.

Generally, scanning acquisition systems such as spatial scanning, spectral scanning or spatio-spectral scanning can obtain hyperspectral images with high spectral and spatial resolution, but require time for the scanning. In contrast, snapshot systems trade-off between spectral and spatial resolution to be able to provide instantaneous and faster acquisition than scanning systems. This way, in non-scanning or snapshot hyperspectral systems the full 3D hyperspectral data cube, with multiple bands per image point, is captured at once, without the need for scanning. While scanning systems, requiring multiple exposures, are more exposed to motion artifacts, a snapshot imager capturing a multispectral image at one single exposure, can better avoid such artifacts. In this respect, the snapshot cameras enable us to target new application domains with moving objects, such as security/object tracking, or medical applications with moving live tissue.
Lapray et al [13] provide a good review of the different technologies used to develop snapshot multispectral and hyperspectral systems. One of the first methods to be used to implement a snapshot spectral imager, limited to 3 or 4 bands, was beam-splitting. Another way to implement snapshot imagers is by means of a lenslet array, which in combination with a filter array inserted in front of the lenslet array or image sensor allows to duplicate and project the image of each lenslet on the corresponding area of the sensor. One example is shown in [14] where a Continuous Variable Filter (CVF) of Delta Film is used together with a microlens array to provide simultaneous snapshot acquisition of 66 bands in the VNIR range (450-880 nm) with a spatial resolution of 400x400 pixels per band. Finally, we can implement a snapshot system by using Multi-Spectral Filter Arrays (MSFA) that integrate multiple filter elements in a mosaic pattern. This results in superpixels, where the pixels for the different wavebands are spatially separated in a mosaic arrangement. The hyperspectral filters are arranged onto individual pixels extending the Bayer colour imaging concept to hyperspectral imaging where video rate acquisition can be reached without dedicated fore-optics or linear scanning. An example of this is shown in our previous work in [15], where snapshot cameras in the visible and near-infrared ranges are showcased. Traditional hyperspectral camera manufacturers such as Specim [16], have also developed more compact and portable hyperspectral cameras while still relying on push-broom technology [17]. In [18] the snapshot camera Cubert UHD 185 Firefly with 125 bands in the 450-950 nm range and a 50x50 pixel resolution has been introduced and evaluated for a remote sensing application, where accurate yield prediction of barley fields is shown. In [19] the authors show another remote sensing application where the same compact snapshot camera achieves comparable NDVI results than a field spectrometer for crop growth monitoring. In [3] the authors give an overview on the currently available Snapshot hyperspectral imagers on the market enabling its adoption by consumer market as well as its expansion in application fields such as medical imaging, forensics, and remote sensing. Snapshot devices such as the Snapshot Mosaic cameras [15] or the PixelCam camera from Pixelteq [20] are discussed. An overview of the different commercial Snapshot camera characteristics and their prices is given, where we can see that hyperspectral cameras are becoming more cost effective. Recent technology advances are proposing as well snapshot cameras in the SWIR range, either based on Acousto-Optic Tunable Filters [21] or by means of dichroic filter integration directly at sensor level, offering then 3 or 4 bands in this range [22]. Our snapshot sensor builds as well on sensor-level custom filter integration, as explained in our previous work [23] and offers a configuration of either 9 or 16 bands in the 1000-1700 nm range.

In general, the development of snapshot cameras has helped increase acquisition speed and reduced the camera size and cost. In this respect, one of the advantages of "on-chip" hyperspectral technology, where filters are monolithically integrated on top of a chip, is that it can potentially be mass-producible, which could considerably reduce the cost of hyperspectral cameras. Another advantage is that cameras can have a smaller form factor since traditional optical elements such as the grating prism are substituted by filters deposited on the sensor. Note that small and light weight cameras are of key importance for UAV remote sensing applications since low weights increase the flight time. Theoretically, a transmission efficiency close to 100% can be expected from thin-film filter technology for CVF [24], [15]. This potentially allows lower integration times and therefore faster acquisition speeds, which helps reach industrial inspection speeds. Finally, Fabry-Perot filters are lower complexity filters in comparison with those offered by the technology in [24]. They offer higher flexibility in terms of filter arrangement and allow implementation of mosaic patterns, but this comes at the cost of reduced out-of-band blocking capabilities [24]. It is important to note, nevertheless, that this is a relatively recent technology, which is still undergoing substantial technological improvements.

2. MULTISPECTRAL SNAPSHOT CAMERAS

Imec currently offers different evaluation systems based on CMOS imagers with monolithically integrated filters in the visual (VIS) and near-infrared (NIR) spectral ranges [25] using CMOS compatible fabrication processes. Future improvements to these fabrication processes include improved etch control and material tuning, and in-line optical monitoring [26], whereby monitoring the transmission of a test glass at a judiciously selected discrete wavelength during deposition, the deposition can be stopped at a precise optical thickness, dynamically compensating deposition rate and optical constant variations to reach a targeted optical performance. This will enable future snapshot images with better controlled peak wavelengths and advanced filter architectures with higher edge steepness and out-of-band-blocking capabilities, such as the double cavity filters shown in Figure 2-1.

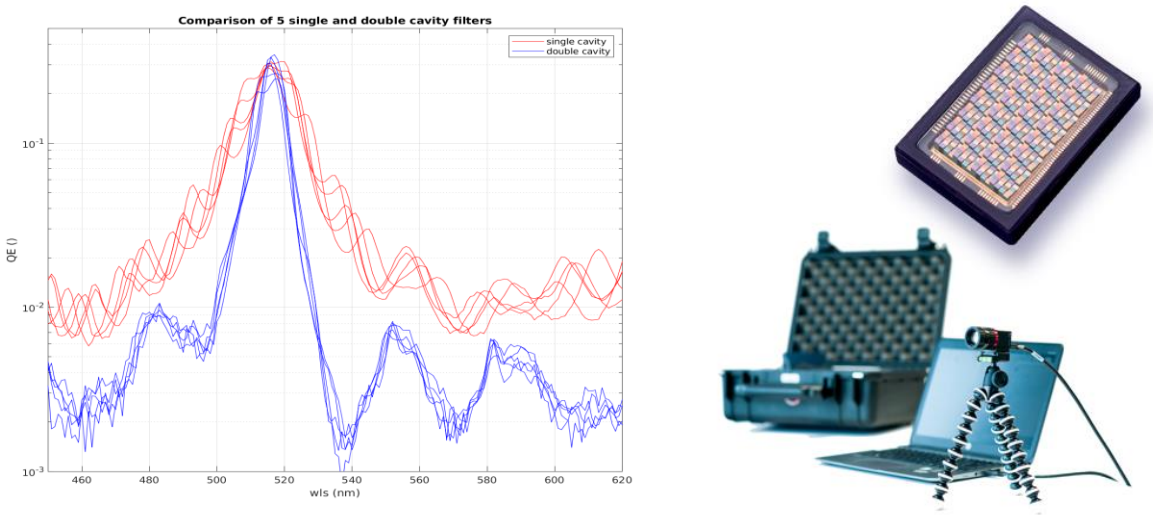

Figure 2-1: Left: Single and double cavity filters using improved fabrication method ([26]) and Right: mosaic snapshot vis/nir camera and sensor

As well as cameras in the VIS and NIR range, a snapshot camera in the short wavelength infrared (SWIR) range (1100-1650 nm) is available. The Imec Mosaic SWIR Snapshot camera has been developed to enjoy the benefits of mosaic snapshot cameras at the expense of a reduced spatial-spectral resolution with respect to the imec Snapscan SWIR camera system [23] with 100 bands in the 1100 to 1650 nm range and a maximum spatial resolution of 1200x 640 pixels. The mosaic sensors are based on 3x3 mosaic filter patterning on an industry-ready SWIR detector. The mosaic patterns are implemented by means of high-transmission Fabry-Pérot interferometers processed using thin-film technology [23].The Mosaic SWIR camera system offers 9 bands in the 1100-1650 nm range at a spatial resolution of 213 x 170 pixels, which

can be up sampled to 633x504 pixels. The lay-out of the 9 bands selected in the 3x3 Mosaic SWIR design is illustrated in Figure 2-2.

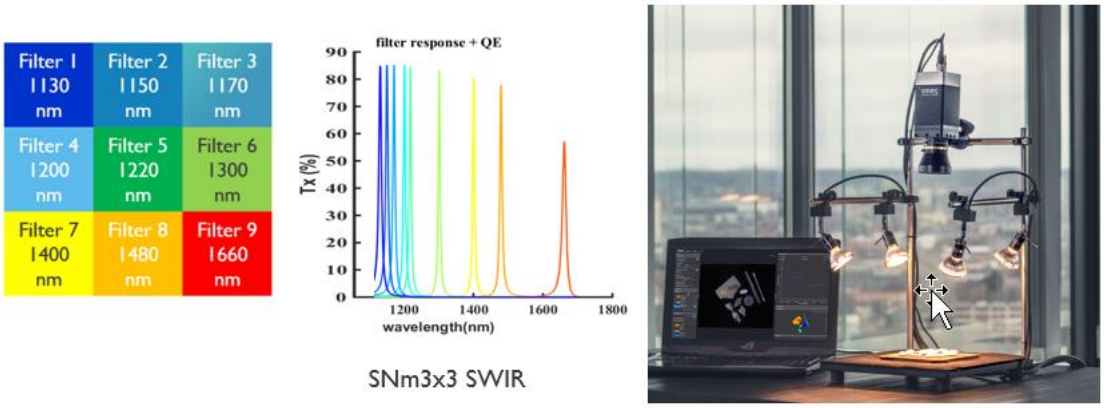

Figure 2-2: Mosaic SWIR camera (right) and the layout of 3x3 SWIR sensor (left)

Table 1 summarizes the specifications of the imec snapshot multispectral cameras in the VIS, NIR and SWIR ranges.

Table 1: Summary of snapshot mosaic camera specifications.

	Band range	**# bands**	**Spatial resolution**	**Dimensions**	**Weight**
Mosaic VIS 1	470-620 nm	16	2040x1080	26x26x31 mm	32 g
Mosaic VIS 2	460-600 nm	16	2040x1080	26x26x31 mm	32 g
Mosaic NIR	665-960 nm	24	2035x1075	26x26x31 mm	32 g
Mosaic RedNIR	600-860 nm	15	2040x1080	26x26x31 mm	32 g
Mosaic SWIR	1100-1650nm	9	633 x 504	65x65x130 mm	260 g

Our snapshot cameras in VIS, NIR and SWIR ranges enable video rates of up to 120 data cubes per second at camera level. First, it is this video rate capability that enables a new range of dynamic applications such as assisted surgery and object tracking, in addition to regular industrial inspection or drone-based inspection. Second, the compact size and low camera weight offers clear advantages for UAV/drone inspection, to comply with space limitations in assisted surgery or to be used as a portable system. Next to this, its ease of use makes it suitable for industrial integration. Finally, the possibility of mass-producible sensors reduces its cost, enables wider adoption of this technology, and bridges the gap towards industrial applications.

3. APPLICATIONS FOR SNAPSHOT MULTISPECTRAL CAMERAS

Snapshot cameras enable a different range of applications where no scanning can be performed such as biomedical or surveillance applications. The fast acquisition of mosaic snapshot cameras makes them particularly useful for these types of dynamic applications since spectral video acquisition at high frame rate can be achieved. Moreover, its ease of use makes it suitable for industrial integration. In this section the work done with these cameras and latest achievements in several application domains are highlighted.

3.1 Agricultural

Within the context of the Smartfarming 4.0 project [27] imec multispectral snapshot cameras have been used for fire blight disease detection in apple and pear plantations. Fruit growers are currently limited to time-consuming, labor-intensive visual inspections of their orchards. Moreover, automated inspection and early detection of infected trees can help them avoid serious economic losses. The designed prototype for this allows to synchronize two snapshot RedNIR cameras (Table 1) and 1 regular color RGB camera along with GPS data. This tractor add-on can be controlled by the driver from the cockpit using a touch screen. Because light conditions are constantly changing during field measurements, a calibration function was also designed in which a reference tile automatically enters sensor's field of view, so that the most optimal settings for the hyperspectral sensors can be determined. Figure 3.1 shows the acquisition setup on the tractor with the multispectral snapshot cameras and the white reference tile. An algorithm was trained to assign pixels from the hyperspectral images to different categories. After the analysis of all images taken with the camera platform, the results of possible presence of fire blight can be displayed on a map. An example of such heat map can be seen in the right side of Figure 3.1. This can immediately give a grower a clear picture in which parts of his orchard there is a risk of infection.

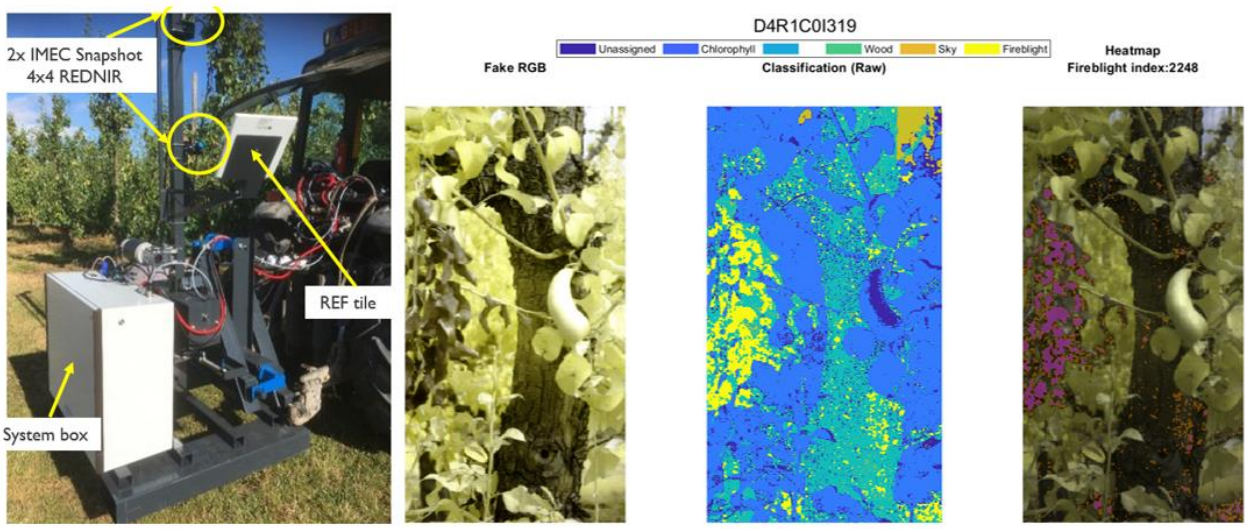

Figure 3-1: Acquisition setup on the tractor (left) and material classification with fireblight infection detection from hyperspectral image.

These compact form factor and light cameras are also being used in remote sensing for Unmanned Aerial Vehicle (UAV) applications [28], [29], [30] as well as in the agro sector [31]. Within smart farming, our compact low weight snapshot cameras are also suitable for UAV inspection. In this respect, most current UAV camera systems are limited by the number of spectral bands (≤10 bands) and are usually not fully integrated with the ground controller to provide a live view of the spectral data. We have developed a compact multispectral camera system with easy control and stable communication. The data processing pipeline enables user to obtain single spectral cubes as well as stitched cube. Our system can help with smart farming. By inspecting crops using hyperspectral cameras, farmers can detect soil quality, water stress and early symptoms of disease. Besides agriculture application, our UAV camera system [30] has also been used for forest surveillance, windmill erosion detection, solar panel maintenance, etc.

3.2 Product quality inspection

Our snapshot multispectral cameras have also been used for product inspection. In [31] both VIS and NIR mosaic cameras were used in combination with neural networks to achieve multi-resolution lawn weed classification. Similarly, in our previous work in [32], [33], both camera types were compared for seed type detection in combination as well with convolutional neural networks.

Within the European project Multiple [34], mosaic snapshot cameras in the VIS and SWIR range are being integrated in different applications for industrial product quality inspection. One of those applications is chocolate gloss estimation, where we have shown that a mosaic VIS camera with 16 bands can achieve high estimation accuracy of the gloss level in chocolate sprinkles. Quality control on the gloss level of chocolate sprinkles is currently done visually by experts, since there is a lack of non-contact automatic tools for gloss estimation suitable for chocolate, and in particular for sprinkles. For this purpose, a snapshot camera in the VIS range was used to image 42 samples of chocolate sprinkles of different gloss levels. A state-of-the-art convolutional neural network (Hybrid3D2D-CNN) is used to perform spatial-spectral analysis, resulting in high accuracy levels of gloss estimation [35]. Spectral data is processed on the cloud and the gloss level estimated per sample by the convolutional network is displayed, as shown in Figure 3-2.

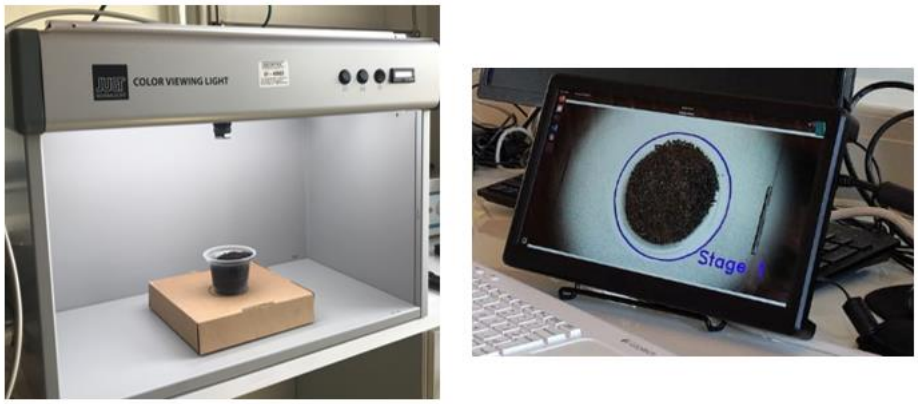

Figure 3-2: Imaging setup with light cabinet and snapshot vis camera (left) and output of neural network as gloss estimation level (right) [35].

Also, within the European project Multiple [34] multispectral SWIR thermography is applied for product quality control by estimating the surface temperature inside a reheating furnace and on steel slabs in a rolling mill. The temperature inside the rolling mill ranges between 700 and 1300ºC. The use of our snapshot multispectral SWIR camera in the 1100-1650 nm range enables here the implementation of different techniques for robust temperature estimation: standard dual-wavelength infrared thermometry or more complex multiwavelength algorithms to compensate for the spectral dependence of emissivity. Figure 3-3 shows the resulting estimated heat maps of the interior of the furnace (left) and of a steel slab.

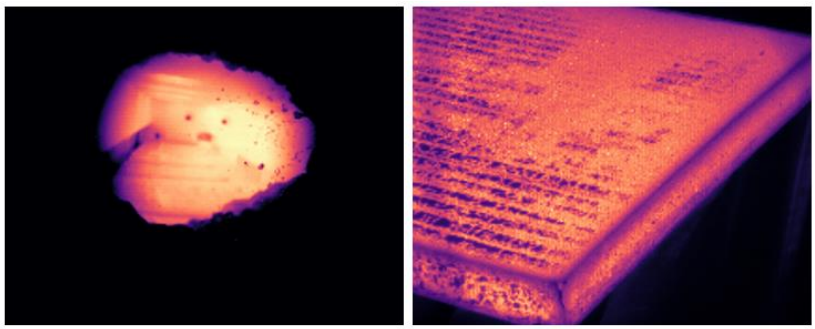

Figure 3-3: Extracted heat maps of interior of the furnace (left) and of a steel slab (right).

3.3 Microscopy for particle contamination exposure assessment

The material discrimination potential of hyperspectral imaging is used within the context of the European project Eximious [36],[37] where occupational particle contamination exposure is assessed to estimate its impact on human health and its correlation with immune system diseases. For this purpose, hyperspectral imaging is used to help develop a quick particle exposure assessment tool in workplaces. To this end, tests for identification of different particle materials with different camera and microscope systems are ongoing. In some of the experimental work the Snapshot SWIR camera with 9 bands is coupled to a Seiwa reflection microscope. Figure 3-4 shows the results achieved for discrimination of silica, polystyrene (PS), and dust particles below 100 µm with hyperspectral imaging in the swir range. The mean reflectance spectra of the three different particle materials are shown and based on per-pixel spectra the particle area is discriminated as one of the three potential materials. The achieved pixel accuracy per material is of 95%, 83% and 98% for polystyrene, dust and silica materials respectively resulting in even higher full particle correct identification. Particles above 10 µm require 10x microscope objective while particles between 1 and 10 µm require a magnification objective of 50x. In our case, polystyrene particles are in the 10-100 µm range while those of silica are below 10 µm but classification is performed per pixel and agnostic of particle size.

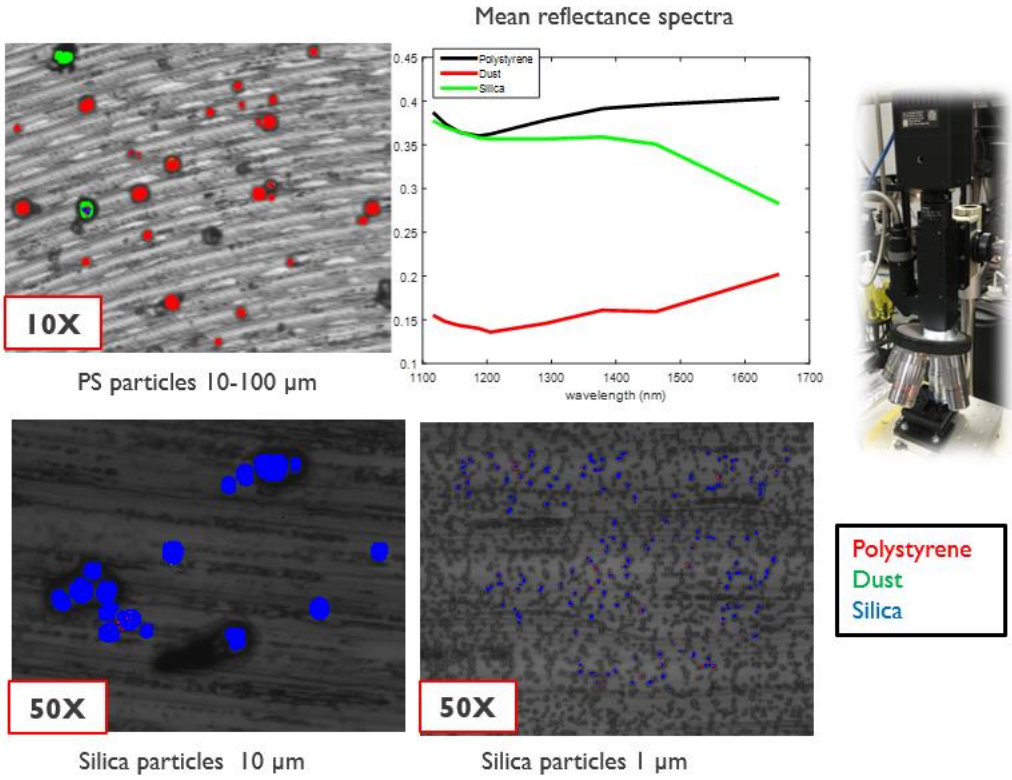

Figure 3-4: Mean spectral signature and classified images of microscopic PS, silica and dust particles inspected with SWIR snapshot camera and reflectance microscope (right).

Material discrimination is currently being extended to a bigger set of particle types. In this respect, hyperspectral imaging can also be interesting for microplastic inspection for both health and environmental impact monitoring. In this respect, the use of snapshot cameras with lower number of bands generates lower amount of data, which can alleviate memory and data processing requirements, especially when deep learning is used.

3.4 Sorting and recycling applications

While some researchers have shown the potential in the 1000-2500 nm range of line scan cameras for plastic and other material sorting [38], [39], [40], none of the works addressed snapshot type of cameras. In our recent work in [41], we showed the potential of the Snapshot SWIR camera for a variety of product sorting applications, more specifically,

plastic, textile, and cardboard sorting. In this work we showed the potential to discriminate with oru Snapshot SWIR camera with high accuracy different type of color plastic samples (PET, PP, HDPE) and different paper and cardboard types. We showed as well accurate discrimination of different textile compositions as pure materials (cotton, wool, polyester, polyamide, silk and viscose) or as textile mixes in different compositions. In the context of the Vision2Reuse project [42], we have extended this work of small plastic portions of different colours to full containers (trays, cups), which are mostly transparent samples. Figure 3-5 below shows the classified images of a variety of transparent trays, lids, and cups of 5 different materials. Pixel-based classification is applied with Linear Discriminant Analysis and Quadratic Discriminant Classifier [43] based on the 9 spectral bands. We can see that high classification accuracy of all objects is achieved, except for minor pixel miss-classifications at the lid edges or specular areas.

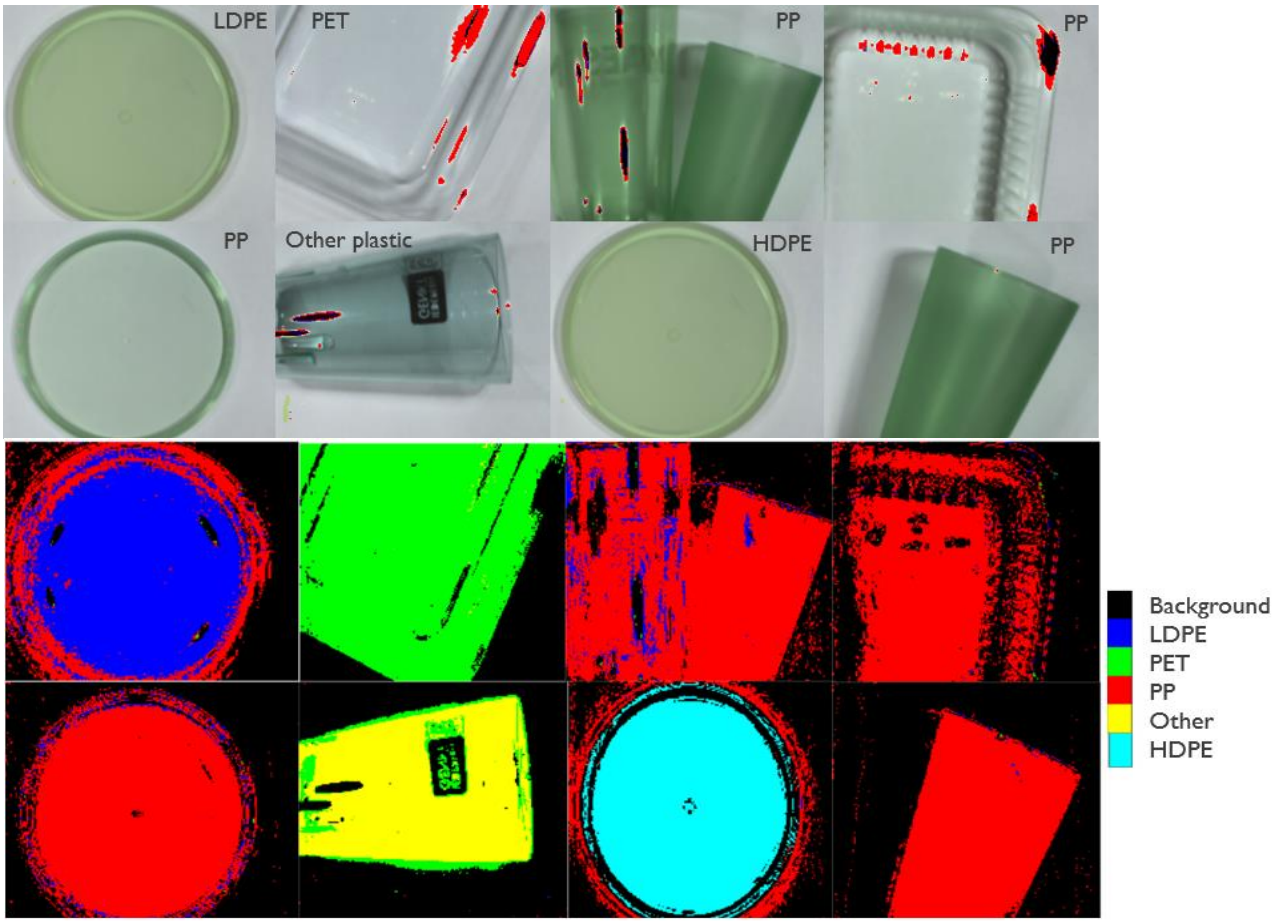

Figure 3-5: False color image (top) and classified images (bottom) of diverse transparent plastic types.

Additionally, we have seen that early detection of water presence can be done with our multispectral SWIR camera. In this sense, early droplets detection is useful to later mold growth on such containers. Real-time material sorting and droplet detection can be done at high speed with our snapshot camera in the with the help of our acquisition software gui. An example of such real-time detection of different tray materials and water presence can be seen in Figure 3-6.

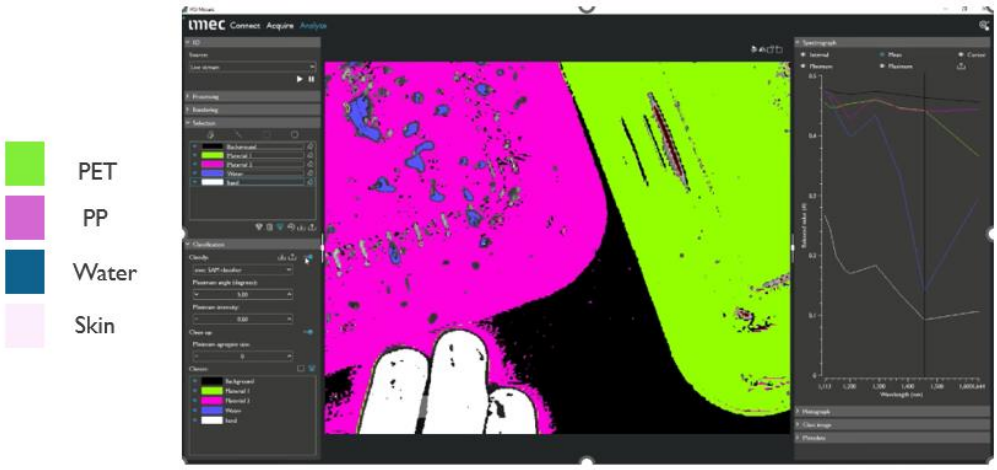

Figure 3-6: HSI gui showing real-time classification of PET and PP plastic containers and water droplet detection

3.5 Object tracking

One important advantage of snapshot multispectral cameras is that they enable the use of multispectral imaging for dynamic scenes where hyperspectral video at high frame rate should be acquired. This makes the use of hyperspectral imaging for object detection and tracking applications possible. In collaboration with the Royal Military Academy [44], [45] one of these applications was explored, namely the detection and tracking of search and rescue personnel under hindered light conditions, such as twilight, white/grey smoke, black smoke, haze and rain. Thanks to the video capabilities of our snapshot cameras, a hyperspectral video shootage of dynamic outdoor scenarios mimicking rescue personnel under low visibility conditions was captured at approximately 25 frames per second with snapshot cameras in the VIS, NIR and SWIR ranges. Figure 3-7 shows the acquired images for the mosaic nir camera (25 bands in the 664-971 nm range) under black smoke (left) and heavy rain (right) scenarios. Based on a two-stage neural network, the proposed method in [45] first exploits the spatial features through object detection and then analyzes the extracted regions using a spectral-spatial pixel-wise algorithm to validate the presence of firefighters. It was observed that in particular bands above 800 nm increase the discrimination in these low visibility conditions and allowed for accurate discrimination of firefighter personnel with respect to policemen or civilians. In Figure 3-7 the resulting bounding boxes for firefighter detection are shown, where green means accepted (firefighter) and red is rejected (policeman or civilian uniform). This way, the algorithm based on the mosaic nir spectral information achieved high accuracy in firefighter detection under a variety of low visibility conditions.

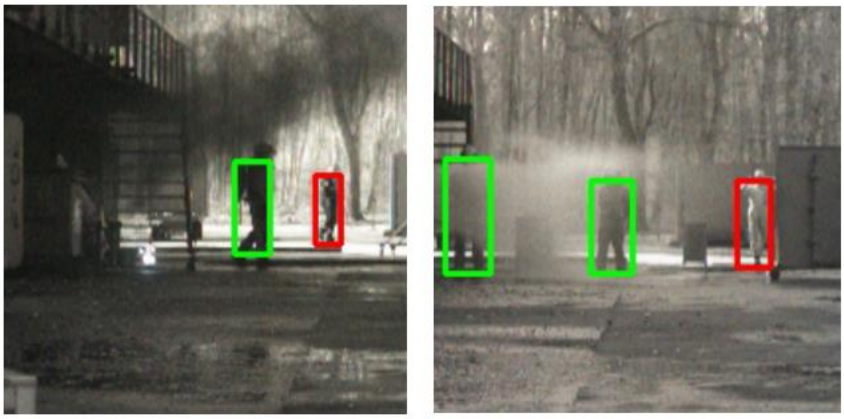

Figure 3-7: Resulting bounding boxes for firefighter detection with mosaic NIR (green: accepted and red: rejected) under the presence of black smoke (left image) and heavy rain (right image)

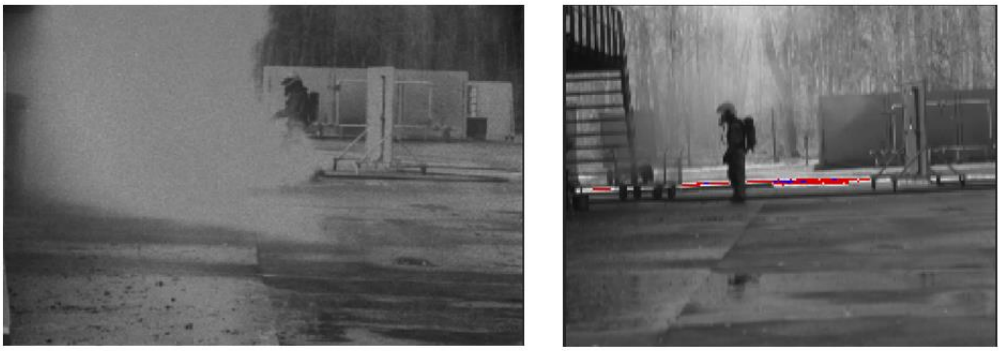

Figure 3-8: Scenes with white smoke, left: VIS range (550 nm band image) and right: SWIR range (1205 nm band image). Unlike VIS range, SWIR range allows visualization of people through white smoke presence.

In Figure 3-8 we can see as well how the snapshot SWIR camera increases considerably discrimination as well with respect to the visible range. The same scene is recorded for all cameras under white/grey smoke presence and while firefighters are easily hidden by smoke in the visual range, inspection in SWIR range (1100-1650 nm) under the same smoke clearly helps detect and visualize the firefighters' presence.

In this context, and to further boost the development of algorithms for object detection and tracking with multispectral imaging snapshot cameras, imec has been co-organizing the object tracking context within the Whispers conference [46]. This has resulted in several related publications [47], [48], [49], where the potential and added value of multispectral snapshot cameras for object tracking has been proven.

3.6 Medical applications

The Snapshot Mosaic cameras enable a different range of applications where no scanning can be performed such as biomedical imaging. Indeed, Mosaic Snapshot cameras have proven to be suitable for medical applications in combination or not with a microscope [54], [50], [52]. For some medical applications, only inspection of the body surface is required (skin and eye imaging, wound monitoring...) This is the case of the work in [50] where our compact Mosaic camera with 16 bands in the visual range was used for retinal imaging at 20fps, enabling potential applications for monitoring of retinal diseases. Similarly, in [51] the same type of Mosaic cameras is used for early Alzheimer detection by retinal inspection.

In this respect, due to the dynamic nature of living tissue and the need for real-time video monitoring capabilities, snapshot multispectral cameras offer great potential for assisted surgery. This can be done with a minimally invasive surgery (based on laparoscopes, endoscopes...) or in open surgery, with possible integration with surgical microscopes or not. To achieve multispectral endoscopy, Luthman [52] coupled a snapshot VIS and a snapshot NIR with an endoscope to discriminate multiple biological components in an ex vivo porcine esophagus. Similarly, Wirkert [53] used both VIS and NIR snapshot cameras with an endoscope to real-time monitor perfusion during a partial nephroctomy intervention. In more open surgery, Pichette et al. [54] used an imec Snapshot VIS camera for real-time monitoring of brain oxygenation during brain surgery. Similarly, after encouraging results with hyperspectral imaging for brain glioma detection and classification [55], [56] the exploration of snapshot spectral cameras for glioma classification is envisaged.

In addition, there is also potential for hyperspectral imaging in the field of in-vitro and histopathology analysis. In the context of particle contamination assessment for the Eximious project [37] some pathology slides are also being inspected to assess whether particle contamination may be present in the tissue. Figure 3-9 shows the images resulting from inspection of a pathology slide of a hematoxylin eosin-stained lymph node tissue with a Leica transmission microscope coupled to the mosaic VIS and NIR multispectral cameras. On the left side of the figure, we can see the corresponding color image created from the VIS camera. The dark purple (hematoxylin stain) structures are mainly cell nuclei, while the various shades of pink (eosin stain) represent the cytoplasm of the cells and other tissue components. On the right-hand side, the false color image coming from the NIR camera at the same tissue location is shown. We can

observe how, below the tissue some potential particle contamination, not observable in the visible range, becomes visible in the NIR range.

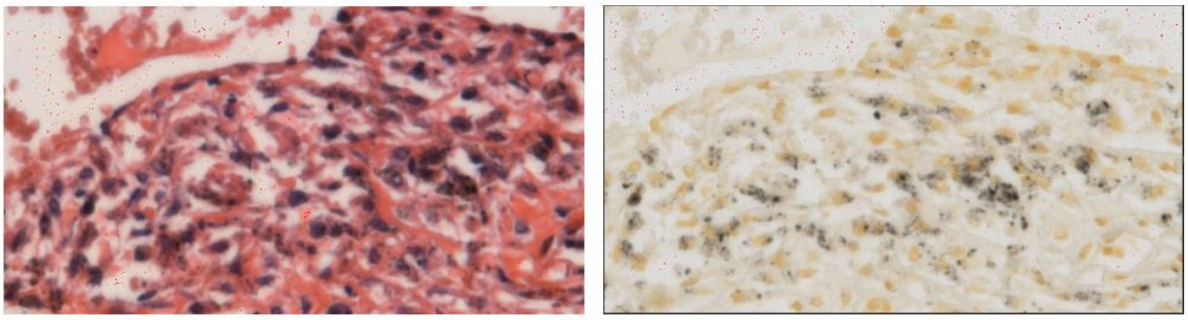

Figure 3-9: Color image of lymph node tissue from multispectral vis camera (left) and corresponding image from multispectral nir camera revealing hidden details.

3.6 Infrastructure inspection

The use of hyperspectral imaging for infrastructure inspection, such as bridges [57], high voltage towers [58], [59], buildings or wood poles [60] is raising higher interest. Today, inspection and cleaning of such infrastructure is typically done by climbing the bridge or tower and having a visual assessment, which is time consuming, costly, and subjective. For this purpose, the use of snapshot multispectral cameras on drones can help automate the inspection and detect early deterioration of the infrastructure, which can result in reduced costs and risks. In [58] a first phase of a project with Elia [61] already established that the corrosion degree of metallic test samples from voltage towers with 2 different coatings was accurately predicted by imec higher resolution hyperspectral cameras in the VNIR and SWIR ranges. In a second phase, we aim to characterize different corrosion degrees in high voltage towers by on-site inspection with drones and snapshot multispectral cameras in the VIS, NIR and SWIR ranges.

4. CONCLUSIONS

Multispectral snapshot cameras enable a wide range of dynamic applications, such as surveillance or assisted surgery, where no scanning can be performed, or spectral video rate acquisition is required. Moreover, snapshot multispectral cameras are paving the way for wider industrial adoption thanks to their ease of use and lower cost. We have presented the latest advances in spectral mosaic snapshot cameras in the visual, near infrared and short wavelength infrared ranges, as well as promising results from their use in a variety of application fields. Some of these application fields where snapshot technology offers new possibilities are biomedical or object tracking but also sorting/recycling, smart farming or product and infrastructure inspection. Since this is a relatively recent technology, it is still undergoing substantial technological improvements with continuous enhancement of their spectral quality. To better meet specific application requirements, other potential future developments could be envisaged such as extensions of the covered wavelength range.

ACKNOWLEDGEMENTS

We want to acknowledge the Eximious project, which has received funding from the European Union's Horizon 2020 research and innovation programme under grant agreement No 874707, as well as the work done in collaboration with Centro Tecnologico Aimen within the project Multiple, with funding from the European Union's Horizon 2020 research and innovation programme under grant agreement No n° 871783. Moreover, we want to acknowledge the research done within the EFRO Vision2Reuse project, with the support from EFRO (Europees Fonds voor Regionale Ontwikkeling), under grant agreement No. 1508 and the work done within the SmartFarming 4.0 project, with the support from VLAIO (Agentschap Innoveren & Ondernemen), research and innovation under grant agreement No. 180503. Finally, we want to thank the collaboration with the Royal Academy of Belgium.

REFERENCES

[1] Elmasry, G., Kamruzzaman, M., Sun, D-W. & Allen, P. (2012). "Principles and Applications of Hyperspectral Imaging in Quality Evaluation of Agro-Food Products: A Review" Critical reviews in food science and nutrition. 2012. 52. 999-1023. 10.1080/10408398.2010.543495.

[2] Khan, M. J., Khan, H.S, Yousaf, A., Khurshid, K. & Abbas, A. (2018). "Modern trends in hyperspectral image analysis: a review". IEEE Access Open Access Journal, Digital Object Identifier 10.1109/ACCESS.2018.2812999, March 2018.

[3] West, M., Grossmann, J., & Galvan, C. (2019). "Commercial Snapshot Spectral Imaging: The Art of the Possible."

[4] Traore, M.K. "Computational Frameworks: Systems, Models and Applications", Book by ISTE Press - Elsevier, 2017. 978-1-78548-256-4

[5] Paoletti, M.E., Haut, J.M., Plaza, J. & Plaza, A. (2019) "Deep learning classifiers for hyperspectral imaging: A review". ISPRS Journal of Photogrammetry and Remote Sensing, Volume 158, December 2019, Pages 279-317

[6] Hagen, N. A., & Kudenov, M. W. (2013). "Review of snapshot spectral imaging technologies". Optical Engineering, 52(9), 090901.

[7] Ortega, S., Guerra, R., Diaz, M., Fabelo, H., Lopez, S., Callico, G-M. & Sarmiento, R. (2019). "Hyperspectral Push-Broom Microscope Development and Characterization". In Special Section on Advanced optical imaging for extreme environments, September 2019. DOI 2019.2937729

[8] Abdlaty, R., Orepoulos, J., Sinclair, P., Berman, R. & Fang, Q. (2018). "High Throughput AOTF Hyperspectral Imager for Randomly Polarized Light". Photonics Journal, 2018, 5(1), 3; https://doi.org/10.3390/photonics5010003

[9] Gonzalez, P., Tack, K., Geelen, B., Masschelein, B., Charle, W., Vereecke, B. & Lambrechts, A. (2016, May) "A novel CMOS-compatible, monolithically integrated line-scan hyperspectral imager covering the VIS-NIR range". In Next-Generation Spectroscopic Technologies IX (Vol. 9855, p. 98550N). International Society for Optics and Photonics. Proc. SPIE 9855, 98550N (2016). https://doi.org/10.1117/12.2230726

[10] Pichette, J., Charle, W., & Lambrechts, A. (2017) "Fast and compact internal scanning CMOS-based hyperspectral camera: the Snapscan" In Photonic Instrumentation Engineering IV (Vol. 10110, p. 1011014). International Society for Optics and Photonics.

[11] Ahlberg, J., Renhorn, I. G., Chevalier, T. R., Rydell, J., & Bergström, D. (2017). "Three-dimensional hyperspectral imaging technique". In Algorithms and Technologies for Multispectral, Hyperspectral, and Ultraspectral Imagery XXIII (Vol. 10198, p. 1019805). International Society for Optics and Photonics, 2017.

[12] Fabricius, H., & Pust, O. (2014) "Linear Variable Filters for Biomedical and Hyperspectral Imaging Applications". In Biomedical Optics (pp. BS3A-42). Optical Society of America, April 2014. DOI: 10.1364/BIOMED.2014.BS3A.42.

[13] Lapray, P-J., Wang, X., Thomas, J.B. & Gouton, P. (2014) "Multispectral Filter Arrays: Recent Advances and Practical Implementation", in Sensors 2014, 14, 21626-21659; doi:10.3390/s141121626

[14] Hubold, M., Berlich, R., Gassner, C., Brüning, R., & Brunner, R. (2018, February). "Ultra-compact micro-optical system for multispectral imaging". In MOEMS and Miniaturized Systems XVII (Vol. 10545, p. 105450V). International Society for Optics and Photonics.

[15] Geelen, B., Blanch, C., Gonzalez, P., Tack, N., & Lambrechts, A. (2015). "A tiny VIS-NIR snapshot multispectral camera". In Advanced Fabrication Technologies for Micro/Nano Optics and Photonics VIII (Vol. 9374, p. 937414). International Society for Optics and Photonics, March 2015.

[16] Herrala, E. (2020), "Guide to selecting hyperspectral instruments", Specim, Spectral Imaging Ltd) Retrieved from https://www.specim.fi/

[17] Behmann, J., Acebron, K., Emin, D., Bennertz, S., Matsubara, S., Thomas, S., Bohnenkamp, D., Kuska, M.T., Jussila, J., Salo, H., Mahlein, A.K. & Rascher, U. (2018). "Specim IQ: Evaluation of a New, Miniaturized Handheld Hyperspectral Camera and Its Application for Plant Phenotyping and Disease Detection". In Sensors 2018, 18(2), 441; https://doi.org/10.3390/s18020441

[18] Oehlschläger, J., Schmidhalter, U., & Noack, P. O. (2018, September). "UAV-based hyperspectral sensing for yield prediction in winter barley". In 2018 9th Workshop on Hyperspectral Image and Signal Processing: Evolution in Remote Sensing (WHISPERS) (pp. 1-4). IEEE.

[19] Bareth, G., Aasen, H., Bendig, J., Gnyp, M. L., Bolten, A., Jung, A., Michels, R. & Soukkamäki, J. (2014, April). "Spectral comparison of low-weight and UAV-based hyperspectral frame cameras with portable

spectroradiometer measurements". In Proceedings of the Workshop on UAV-basaed Remote Sensing Methods for Monitoring Vegetation (Vol. 94, pp. 1-6). Geographisches Institut der Universität zu Köln-Kölner Geographische Arbeiten.
[20] "PixelCam, OEM Multispectral Imaging Camera". Retrieved from https://www.acalbfi.com/uk/Imaging-for-Science-and-Industry/Hyperspectral-Imager/p/OEM-Multispectral-Imaging-Camera/0000003FJW. https://www.pixelteq.com
[21] https://www.brimrose.com/aotf-hsi-resource-center
[22] http://www.rktech.hu/dokumentaciok/PixelTeq/PixelCam.pdf
[23] Gonzalez, P., Pichette, J., Vereecke, B., Masschelein, B., Krasovitski, L., Bikov, L., & Lambrechts, A. (2018, May). "An extremely compact and high-speed line-scan hyperspectral imager covering the SWIR range". In Image Sensing Technologies: Materials, Devices, Systems, and Applications V (Vol. 10656, p. 106560L).
[24] Pust, O. (2016). "Innovative Filter Solutions for Hyperspectral Imaging". In Optik & Photonik. https://onlinelibrary.wiley.com/doi/pdf/10.1002/opph.201600012
[25] Imec hyperspectral cameras, https://www.imechyperspectral.com/en/cameras
[26] Geelen, B. & Tack, K. "A new compact snapshot multispectral mosaic imager with an improved deposition process", (2022, March). In Integrated Optics: Devices, Materials, and Technologies XXVI (Vol. 12004, pp. 180-186). SPIE.
[27] Proeftuin Smart Farming 4.0 | Drones veroveren onze velden (industrie40vlaanderen.be)Industrie 4.0 | Ontdek de proeftuinen van de Vlaamse overheid (industrie40vlaanderen.be)
[28] Lanaras, C. (2018). "Enhancing the Spectral and Spatial Resolution of Remote Sensing Images" (Vol. 122). ETH Zurich.
[29] Goossens, T., Van De Vijver, R., Mertens, K., Saeys, W., Lootens, P., Somers, B., ... & Van Hoof, C. (2018). "System characterization of a snapshot mosaic spectral camera for UAV applications in agriculture". In Hyperspectral Imaging & Applications Conference, October 2018.
[30] Li, Y., Masschelein, B., Vandebriel, R., Vanmeerbeeck, G., Luong, H., Maes, W., ... & Lambrechts, A. (2022, March). Compact VNIR snapshot multispectral airborne system and integration with drone system. In Photonic Instrumentation Engineering IX (Vol. 12008, pp. 228-231). SPIE.
[31] Farooq, A., Jia, X., Hu, J., & Zhou, J. (2019, September). "Knowledge Transfer via Convolution Neural Networks for Multi-Resolution Lawn Weed Classification". In 2019 10th Workshop on Hyperspectral Imaging and Signal Processing: Evolution in Remote Sensing (WHISPERS) (pp. 01-05). IEEE.
[32] Blanch-Pérez-del-Notario, C., Saeys, W., and Lambrechts, A. (2019, September). "Convolutional neural networks for heterogeneous ingredient discrimination with hyperspectral imaging". In 2019 10th Workshop on Hyperspectral Imaging and Signal Processing: Evolution in Remote Sensing (WHISPERS) (pp. 1-6). IEEE.
[33] Blanch-Pérez del Notario, C., López-Molina, C., Lambrechts, A. and Saeys, W. "Hyperspectral system trade-offs for illumination, hardware and analysis methods: a case study of seed mix ingredient discrimination", in Journal of Spectral Imaging 9, a16 (Dec 2020). https://doi.org/10.1255/jsi.2020.a16.
[34] MULTIPLE - The future of photonics-based process optimisation (multipleproject.eu)
[35] Ródenas-Perez, P., Blanch-Perez-del-Notario, C., Lopez-Lopez, E., & Mendez-Rial, R. "Gloss estimation of chocolate sprinkles with hyperspectral imaging". in EFFoST International Conference (2022).
[36] Mapping Exposure-Induced Immune Effects: Connecting the Exposome and the Immunome | EXIMIOUS Project | Fact Sheet | H2020 | CORDIS | European Commission n.d. https://cordis.europa.eu/project/id/874707 (accessed July 7, 2022).
[37] Ronsmans, S., Hougaard, K. S., Nawrot, T. S., Plusquin, M., Huaux, F., Cruz, M. J., ... & Hoet, P. H. (2022). The EXIMIOUS project—Mapping exposure-induced immune effects: connecting the exposome and the immunome. In Environmental Epidemiology, 6(1).
[38] "T4T project". https://ec.europa.eu/environment/ecoinnovation/projects/en/projects/t4t
[39] Chen, H., Tan, C., & Lin, Z. (2020). "Quantitative Determination of the Fiber Components in Textiles by Near-Infrared Spectroscopy and Extreme Learning Machine". Analytical Letters, 53(6),844-857.
[40] Mäkelä, M., Rissanen, M., & Sixta, H. (2020). "Machine vision estimates the polyester content in recyclable waste textiles", Resources, Conservation and Recycling, 161, 105007.
[41] Blanch-Perez-del-Notario, C., Luthman, S., Lefrant, R., Gonzalez, P., & Lambrechts, A. (2022, May). "Compact high-speed snapshot hyperspectral imager in the SWIR range (1.1-1.65 nm) and its potential in sorting/recycling industry". In *Algorithms, Technologies, and Applications for Multispectral and Hyperspectral Imaging XXVIII* (Vol. 12094, pp. 47-55). SPIE.

[42] VISION2REUSE | Pack4Food
[43] Naes, T., Isaksson, T., Fearn, T. & Davies, T. (2004). "A User-Friendly Guide to Multivariate Calibration and Classification". NIR Publications.
[44] Royal Military Academy (RMA), Brussels, Belgium. https://www.rma.ac.be/
[45] Antson, L., Vandenhoeke, A., Simoni, M., Hamesse, C. & Luong, H. "Detection and tracking of search and rescue personnel under hindered light conditions using hyperspectral imaging". In 12th Workshop on Hyperspectral Imaging and Signal Processing: Evolution in Remote Sensing (WHISPERS). IEEE
[46] https://www.hsitracking.com/
[47] Su, N., Liu, H., Zhao, Ch., Yan, Y., Wang, J. and Hei, J. "A transformer-based three-branch siamese network for hyperspectral object tracking", in Whispers conference 2022.
[48] Wang, Y., Liu, Y., Zhang, G., Su, Y., Zhang, S. and Mei, S. "Spectral-spatial-aware transformer fusion network for hyperspectral object tracking", in Whispers conference 2022.
[49] Zhang, Y., Want, F., Wei, B. and Li, L. "A fast hyperspectral object tracking method based on channel selection strategy", in Whispers conference 2022.
[50] Li, H., Liu, W., Dong, B., Kaluzny, J. V., Fawzi, A. A., & Zhang, H. F. (2017). "Snapshot hyperspectral retinal imaging using compact spectral resolving detector array". Journal of Biophotonics, 10(6-7), 830-839. 2017.
[51] Lemmens, S., Van Craenendonck, T., Van Eijgen, J., De Groef, L., Bruffaerts, R., de Jesus, D. A., ... & Stalmans, I. (2020). Combination of snapshot hyperspectral retinal imaging and optical coherence tomography to identify Alzheimer's disease patients. Alzheimer's research & therapy, 12(1), 1-13.
[52] Luthman, A. S., Waterhouse, D. J., Ansel-Bollepalli, L., Yoon, J., Gordon, G. S., Joseph, J., ... & Bohndiek, S. E. (2018). "Bimodal reflectance and fluorescence multispectral endoscopy based on spectrally resolving detector arrays". Journal of Biomedical Optics, 24(3), 031009.
[53] Wirkert, S. J. (2018). Multispectral Image Analysis in Laparoscopy-A Machine Learning Approach to Live Perfusion Monitoring (Doctoral dissertation, KIT-Bibliothek).
[54] Pichette J, Laurence A, Angulo L, Lesage F, Bouthillier A, Nguyen DK, Leblond F. Intraoperative video-rate hemodynamic response assessment in human cortex using snapshot hyperspectral optical imaging. Neurophotonics. 2016 Oct;3(4):045003. doi: 10.1117/1.NPh.3.4.045003. Epub 2016 Oct 12. PMID: 27752519; PMCID: PMC5061108.
[55] Vandebriel, R., Luthman, S., Vunckx, K., Jayapala, M. Charle, W., Solie, L., de Vleeschouwer, S., Giannantonio, T., Alperovich, A. and Zhang, X. "Integrating Hyperspectral Imaging in an Existing Intra-Operative Environment for Detectionof Intrinsic Brain Tumors", to appear in SPIE Photonics 2023.
[56] Giannantonio, T., Alperovich, A., Semeraro, P., Atzori, M., Zhang, X. Luthman,S., Vandebriel, R., Jayapala, M., Solie, L. and de Vleeschouwer, S, "Fast Intra-operative Brain Cancer Detection with Neurally Optimized Hyperspectral Imaging" to appear in SPIE Photonics 2023.
[57] Huynh, C. P., Mustapha, S., Runcie, P., & Porikli, F. (2015). Multi-class support vector machines for paint condition assessment on the Sydney Harbour Bridge using hyperspectral imaging. Struct. Monit. Maint, 2(3), 181-197.
[58] Zahiri, Z., Luong, H., Platisa, L., Vandebriel, R., Jayapala, M, Mangialetto, F and Scheunders, P. "Detecting and characterizing corrosion on high voltage metallic towers using hyperspectral imaging", in Whispers 2022.
[59] Zahiri, Z., Lamberti, A. Wielant, J and Scheunders, P. "Characterization of corrosion products on carbon steel using hyperspectral imaging in short-wave infrared (SWIR)", in Whispers 2022.
[60] Jochmsen, A., Alfredsen, G. and Burud, I. "Hyperspectral imag analysis of scots pine sapwood affected by decay fungi", in Whispers conference 2022.
[61] Elia: Belgian's Electricity System Operator